

Conceptual Design of a Twin-Boom Fixed-Wing VTOL UAV

A Project Report Submitted
in Partial Fulfillment of the Requirements
for the Degree of
BACHELOR OF TECHNOLOGY

by
Vivek T
(150826)



Department of Aerospace Engineering
INDIAN INSTITUTE OF TECHNOLOGY
KANPUR

Kanpur 208016, INDIA

July 2019

Abstract

VTOL UAVs are unmanned airborne vehicles capable of take-off and landing in several different space-constrained environments. A good VTOL UAV is capable of executing vertical climb and descent, hover at a certain altitude, attain a specific ceiling with ease and perform fairly demanding maneuvering flight without losing stability or control. It should also be able to smoothly transition from the VTOL mode to the fixed-wing mode and vice versa. This array of complex motion seeks a careful and well thought out design methodology.

This report describes the design of a twin-boom fixed-wing VTOL UAV. From the mission requirements, a preliminary design was obtained and through performance, stability and control analysis, the design was further optimized. The flight envelope of the UAV was studied along with the consideration of wind and gust effects. The effects of installation of a SATCOM as well as a parachute recovery system is also studied

Keywords: Fixed-wing, VTOL

Acknowledgements

First and foremost, I would like to thank my guide, Dr Ajoy Kanti Ghosh for having suggested the topic of my project and for his constant support and guidance, without which I would not have been able to attempt this project. Thanks are also due to Qazi Salahuddin for helping me throughout the project. Finally I would like to thank my parents for their constant encouragement and motivational support.

Certificate

It is certified that the work in this report titled "Conceptual Design of a Twin-Boom Fixed-Wing VTOL UAV" is the original work done by Vivek T (150826) and has been carried out under our supervision.

Ajoy Kanti Ghosh
Project Supervisor
Department of Aerospace Engineering
Indian Institute of Technology Kanpur
Kanpur 208016



Contents

1	Introduction	1
1.1	Introduction	1
1.2	Mission requirements	1
2	Comparative Analysis	3
3	Preliminary design	7
3.1	Airfoil Selection	7
3.2	Weight Estimation	8
3.2.1	Fuel and Empty Weight	8
3.2.2	Individual Component Weights	9
3.3	Drag Polar	11
3.3.1	Wetted Areas	12
3.3.2	Zero-Lift Drag Coefficient	13
3.3.3	Overall C_{Do}	15
3.4	Geometric Sizing	16
3.4.1	Wing Sizing	16
3.4.2	Fuselage Design	17
3.4.3	Horizontal Tail Sizing	18
3.4.4	Vertical Tail Sizing	18
3.5	Power Plant Selection	19
3.6	Propeller Selection	20
3.7	Control Surface Sizing	21
3.8	Stability and Control Derivatives	22
3.9	Trim Analysis	23
4	Spin Recovery	27
4.1	Introduction	27
4.2	Method I	27
4.3	Method II	29

5	Parachute Recovery System Design	30
5.1	Introduction	30
5.2	Material selection	30
5.3	Design	31
5.4	Other Considerations	32
6	SOTM Installation	33
7	Vn diagram, Wind and gust effects	36
7.1	Flight Envelope	36
7.2	Wind and Gust effects	37

Chapter 1

Introduction

1.1 Introduction

UAVs are being extensively manufactured by a large number of companies as they have already proven their worth in a variety of fields like military, search and rescue, crop monitoring, border protection, disaster response [5], etc. Their ability to make seemingly difficult maneuvers and access hard-to-reach places have made them a useful device in the modern world. By having the ability for vertical take-off and landing, the aircraft can avoid the need for ground space to be utilized as runways.

VTOL UAVs can be divided into four categories: Tilt-rotor, tilt-wing, tail-sitter, and dual-system (e.g. quad plane). They vary in their design complexities with the tailsitter configuration being the simplest possible implementation. This is partly because they don't require extra actuators for the process of transition [4].

In this project, based on the mission requirements, an optimal design of a twin-boom fixed-wing VTOL UAV is achieved. It involves the geometric sizing of the wing, horizontal and vertical tail and fuselage, weight estimation of different components of the aircraft, selection of the power plant and the propellers, sizing of control surfaces, and analysis of the aircraft performance, control and stability.

1.2 Mission requirements

The fixed-wing VTOL UAV was to be designed for a maximum take off weight of 150 kg. Endurance of 6 hrs at a cruising altitude of 5

km was to be expected from the design. The model was supposed to carry a maximum payload of 50 kg and it was required to have a maximum speed of 25-30 m/s. The designed aircraft was also required to incorporate a twin boom structure.

Chapter 2

Comparative Analysis

Before delving into the design phase, a historical perspective was adopted where in existing aircraft with similar elements of the mission requirement were taken into account and analyzed. It aided in forming a basic understanding of the range of aircraft parameters that would typically be encountered in the design phase. This in turn helps in making better decisions, verify the validity of subsequent calculations, correct erroneous results and so on.

The selection of aircraft for comparative study was primarily based on its type and weightclass. Fixed-wing UAVs with a tail-boom configuration and gross weight of about 150 kg were given preference. The following UAVs were hence shortlisted:

- Zala 421-20
- Aerostar (ADS)
- Aisheng ASN 206
- Primoco UAV
- DRDO Kapothaka
- Aeroland AL-150
- H150L XY Aviation
- Sojka III
- AAI RQ-7 Shadow
- AAI RQ-2 Pioneer

- Dronetech AV-1 Albatross
- Yabhon-RX
- ANTEX-M X03
- BAE Systems Phoenix
- IAI Scout
- Innocon MiniFalcon II
- BAE Systems Kingfisher 2
- EADS 3 Sigma Nearchos

Some of the immediate qualitative properties that are observable from the above group of aircraft includes a preference for high wing configuration, pusher propulsion, boom-mounted tail or V-tail configuration, very little to no wing dihedral, lack of wing sweep etc. The quantitative data is represented in Table 2.1 and 2.2 and includes overall dimensions, weights, performance and engine power of the UAVs.

Table 2.1: Comparative Data Sheet - I

UAV	Overall dimensions				Weights	
	Length (m)	Wingspan (m)	Height (m)	Payload (kg)	Empty weight (kg)	Gross weight (kg)
Zala 421-20	5.5	6	1	50		200
Aerostar	4.5	8.7	1.2	50		230
ASN 206	3.8	6	1.4	50		222
Primoco UAV	3.7	4.9	1.25	30		150
Kapothaka	3.67	4.5				130
AL-150	3.5	8	1.1	40	50	150
H150L	3.28	5.9	0.98	30	73	130
Sojka III	3.78	4.12				145
AAI RQ-7 Shadow	3.4	4.3	1	43	84	170
AAI RQ-2 Pioneer	4.3	5.15	1			205
AV-1 Albatross	3	5.4			70	125
Yabhon-RX	3.75	5.8	1	50	70	160
ANTEX-M X03		7		30		150
BAE Phoenix	3.8	5.6		50		175
IAI Scout	3.68	4.96	0.94	38	96	159
MiniFalcon II	4.2	5.5		35		150
BAE Kingfisher 2	4.2	4.23		22		121
Nearchos	3.95	5.1	1.15		60	110
Tadiran Mastiff	3.3	4.25	0.89	37	72	138

Table 2.2: Comparative Data Sheet - II

UAV	Max speed (km/h)	Cruise speed (km/h)	Range (km)	Endurance (h)	Service ceiling (m)	Power (hp)
Zala 421-20			400	8	3700	
Aerostar	200	111.12	250	12	5500	38
ASN 206	210		150	4	6000	
Primoco UAV	180	125	1500	10	3000	30
Kapothaka	180			1.5	3000	26
AL-150	140	110	750	8	5000	32
H150L	160	120		4	5000	22
Sojka III	180	130	100			
AAI RQ-7 Shadow	200	130	109	6	4600	38
AAI RQ-2 Pioneer			180		4600	38
AV-1 Albatross	148	120.38		35		
Yabhon-RX	240	204		6	5500	50
ANTEX-M X03	130			15	4500	22
BAE Phoenix	166	85		5	2800	25
IAI Scout	176			7.5	4600	22
MiniFalcon II		222.24	200	15	5486	
BAE Kingfisher 2		176	95	3		38
Nearchos	220			12	7000	38
Tadiran Mastiff	185			7.5	4480	

Chapter 3

Preliminary design

3.1 Airfoil Selection

Choosing an appropriate airfoil for the wing is a very crucial and fundamental point of the whole journey of the conceptual design. It plays a significant role in the overall aerodynamic efficiency, cruise speed, and handling qualities of the UAV. Designing an airfoil from scratch is a complex and time-consuming process and hence the next best option available is used i.e. to select an airfoil from the plethora of data readily available. Even though it may not be the perfect choice, it suffices to suit the requirements that the UAV has to meet.

The following characteristics are checked while making a proper airfoil selection: [2]

- Cd shape of the usable Cl region
- Behavior of the drag bucket for laminar airfoils (high Re no)
- Stall behavior - sharp vs gradual
- Pitching-moment coefficient - can drive trim drag
- Compatibility with flaps
- Effectiveness with control surfaces
- Thickness to chord - for structures and internal volume
- Ability to operate over entire flight envelopes (Re, Mach)
- Ease of construction (Thin, cusped trailing edges are hard to build)

From the surveyed models of UAVs, the average wingloading was found to be 28.95 kg/m^2 and it ranges between 18.75 and 39.81 kg/m^2 .

This value was used in the further calculations to obtain the ideal lift coefficient and maximum lift coefficient of the airfoil required for the wing. The following relations were used to reach the results:

$$C_{L_{cruise}} = \frac{W/S}{\frac{1}{2}\rho V_{cr}^2} = \frac{20 \times 9.8}{\frac{1}{2} \times 0.736 \times 27.5^2} = 0.70 \quad (3.1)$$

$$C_{L_w} = \frac{C_{L_{cruise}}}{0.95} = 0.74 \quad (3.2)$$

$$C_{l_i} = \frac{C_{L_w}}{0.9} = 0.82 \quad (3.3)$$

$$C_{L_{max}} = \frac{W/S}{\frac{1}{2}\rho_o V_s^2} = \frac{20 \times 9.8}{\frac{1}{2} \times 1.225 \times 23^2} = 1.49 \quad (3.4)$$

$$C_{L_{maxw}} = \frac{C_{L_{max}}}{0.95} = 1.58 \quad (3.5)$$

$$C_{l_{max}} = \frac{C_{L_{maxw}}}{0.9} = 1.66 \quad (3.6)$$

$$C_{l_{max}} = C_{l_{maxgross}} \quad (3.7)$$

$$(3.8)$$

$C_{l_{max}}$ was taken as $C_{l_{maxgross}}$ by assuming that there are no flaps present on the wing. This was to avoid the complication of the preliminary design analysis. The operating regime of Reynold's number was calculated from the following relation while assuming the characteristic length to be 1 m for the wing mean chord.

$$Re = \rho V L / \mu = 1.24 \times 10^6 \quad (3.9)$$

Based on the calculated ideal lift coefficient and maximum lift coefficient, an airfoil was chosen with similar characteristics. NACA series of airfoils are the most readily available and has a wide variety to choose from. Among the different series, 6-digit series were preferred because of the higher laminar flow over the airfoil, ease of construction and being applicable to low-subsonic models of UAV. After shortlisting a few airfoils and analyzing their C_L vs α , C_D vs α and C_m vs α plots in the calculated Reynold's number regime, *NACA 64₃418* was chosen.

3.2 Weight Estimation

3.2.1 Fuel and Empty Weight

The design process continued with a preliminary weight estimation which involved the evaluation of fuel weight fraction and empty weight

fraction. The expression for total weight of the aircraft is -

$$W_{TO} = W_{payload} + W_{fuel} + W_{crew} + W_{empty} \quad (3.10)$$

$$W_{TO} = 150 \text{ kg (given)}$$

$$W_{payload} = 50 \text{ kg (given)}$$

$$W_{crew} = 0 \text{ since the aircraft is unmanned.}$$

W_{fuel} was estimated using the endurance equation for propeller-type aircrafts [6].

The mass fraction of fuel is obtained from

$$MF_{fuel} = 1 - \exp\left(\frac{-EVBSFC}{\frac{L}{D}\eta_p}\right) \quad (3.11)$$

By assuming the brake specific fuel consumption (BSFC) to be 0.78 lb/hp-hr (or 4649.7 g/kW-hr), $\frac{L}{D}$ to be 14, and η_p to be 0.7, the value of MF_{fuel} was calculated to be 0.072. This was used to determine the fuel weight using the relation

$$W_{fuel} = MF_{fuel}W_{TO} \quad (3.12)$$

and the fuel weight came out to be 11.25 kg.

Empty weight was found using

$$W_{empty} = W_{TO} - W_{fuel} - W_{payload} - W_{crew} \quad (3.13)$$

and empty weight fraction from

$$MF_{empty} = \frac{W_{empty}}{W_{TO}} \quad (3.14)$$

The results of the preliminary weight calculations are listed in Table 1.

3.2.2 Individual Component Weights

The individual component weights were then estimated starting with the wing weight. For that purpose, an ultimate load factor $N_z = 5$ was assumed.

Table 3.1: Summary of preliminary weight estimation results

Maximum take-off weight	150 kg
Fuel weight	11.25 kg
Empty weight	88.75 kg
Maximum payload weight	50 kg
Crew weight	0 kg

Thickness-to-chord ratio at the wing root ($\frac{t}{c_{root}}$) = 0.179 for the chosen wing airfoil.

Gerard's formula was used for wing weight estimation [2],

$$W_{wing} = 0.0038(N_z W_{TO})^{1.06} AR^{0.38} S^{0.25} (1 + \lambda)^{0.25} \left(\frac{t}{c}\right)^{-0.14} \quad (3.15)$$

Using Cessna equation for horizontal tail weight estimation,

$$W_{HT} = \frac{3.184 W_{TO}^{0.887} S_{HT}^{0.101} AR_{HT}^{0.138}}{57.5 t_{root_{HT}}^{0.223}} \quad (3.16)$$

where W_{TO} is in pounds.

Fuselage length was obtained from

$$l_{FUS} = 0.538b + 1.66 \quad (3.17)$$

which was calculated to be 5.43 m.

For fuselage weight estimation the following relation was used:

$$W_{FUS} = 0.5257 F_{MG} F_{NG} F_{Pres} F_{VT} F_{Matl} L_{struct}^{0.3796} (W_{carried} N_z)^{0.4863} \left(\frac{1.3V}{100}\right)^2 lb \quad (3.18)$$

Here,

$F_{MG} = 1.07$ assuming the main gear to be on the fuselage

$F_{NG} = 1.04$ assuming the nose gear to be on the fuselage

$F_{Pres} = 1$ as the UAV has an unpressurized fuselage

$F_{VT} = 1$ as the vertical tail weight was not to be included in the fuselage weight.

$F_{Matl} = 1$ as the material factor for a metallic fuselage was 1.

L_{struct} is the structural length of the fuselage in feet.

$W_{carried}$ is the weight of the components carried within the structure in pounds [2].

Total weight of the booms were determined using the relation:

$$W_{boom} = 0.14L_{boom}W_{cant} \text{ lb} \quad (3.19)$$

Here L_{boom} is the total boom length between the attachment points of the wing and the tail in feet and W_{cant} is the total cantilevered weight in pounds which includes the tail and any systems contained within the tails [2].

The avionics, instrumentation, and communication weights were calculated as

$$W_{avion} = W_{avionics} + W_{inst} + W_{comms} + W_{wiring} \quad (3.20)$$

where $W_{avionics}$ is the avionics weight, W_{inst} is the instrumentation weight, W_{comms} is the communication system weight, and W_{wiring} is the wiring harness weight. The basic avionics weight that can be used at the beginning of the conceptual design is given by

$$W_{avion} = f_{avion}W_{TO} \quad (3.21)$$

The factor f_{avion} varies from 0.06 to 0.16. A nominal value of 0.1 was considered here to obtain the basic avionics weight as $W_{avion} = 15$ kg.

Summary of the individual component weights of the aircraft is listed in Table 2.

Table 3.2: Summary of component weight estimation results

Wing weight	21.43 kg
Horizontal tail weight	9.10 kg
Total empennage weight	14.57 kg
Total boom weight	6.68 kg
Avionics weight	15kg

3.3 Drag Polar

Drag polar is expressed using the following equation:

$$C_D = C_{D_o} + kC_L^2 \quad (3.22)$$

Since the equation is of the form $y = a + bx^2$, the plot of C_L vs C_D will be parabolic in nature. The evaluation of C_{D_o} is executed via the "build up" technique in which C_{D_o} is thought to have contribution from individual components of the aircraft. As such the total C_{D_o} is expressed as the summation of C_{D_o} of all contributing components.

$$C_{D_o} = C_{D_{of}} + C_{D_{ow}} + C_{D_{oh}} + C_{D_{ov}} + C_{D_{oLG}} + \dots \quad (3.23)$$

where $C_{D_{of}}$, $C_{D_{ow}}$, $C_{D_{oh}}$ and $C_{D_{ov}}$ refers to the contribution of zero lift drag coefficient of fuselage, wing, horizontal tail and vertical tail respectively.

3.3.1 Wetted Areas

Planform wetted area

The relation used to make a preliminary calculation of planform wetted area assumes that the wing is straight and tapered.

$$S_{wet_{plf}} = 2S_{exp.plf} \left(1 + \frac{0.25(t/c)_r(1 + \tau\lambda)}{1 + \lambda} \right) \quad (3.24)$$

Thickness to chord ratio for NACA 64418 is 0.18. τ in here is defined as:

$$\tau = \frac{(t/c)_r}{(t/c)_t} \quad (3.25)$$

Since the wing uses the same airfoil across the span, $\tau = 1$. Evaluating the equation 3.24 gives $S_{wet_{plf}} = 14.26 \text{ m}^2$

Fuselage wetted area

Roskam recommends a fuselage fineness ratio of 8 for a subsonic aircraft. The length of the fuselage was approximated to be 2.75 m. Fuselage fineness ratio is defined as:

$$\lambda_f = \frac{l_f}{D_f} \quad (3.26)$$

where l_f is the length of the fuselage and D_f is its maximum diameter. Using this relation, maximum equivalent diameter was evaluated to be 0.34 m and the wetted fuselage area followed from the relation:

$$S_{wet_{fus}} = \pi D_f l_f \left(1 - \frac{2}{\lambda_f} \right)^{\frac{2}{3}} \left(1 + \frac{1}{\lambda_f^2} \right) \quad (3.27)$$

Similar procedures were used to evaluate the wetted surface areas of the empennage and the booms. The results are summarized in Table 3.3. The total wetted surface area was obtained by summing all the above evaluated areas. It came out to be about $22.7 m^2$ or $249.4 ft^2$. In order to verify the correctness of the obtained answer, an alternative method was used to evaluate the total wetted surface area based on a take-off weight and wetted area correlation:

$$\log_{10}S_{wet} = c + d\log_{10}W_{TO} \quad (3.28)$$

where S_{wet} is the wetted area, W_{TO} is the take off weight in lbs, and c and d are regression line coefficients. For single engine propeller driven airplanes, c is taken as 1.0892 and d to be 0.5147. The above equation yields S_{wet} to be $243.16 ft^2$ which is close to the value that was obtained using the previous method.

Table 3.3: Summary of wetted areas

Component	Wetted area (m^2)
Planform	14.26
Fuselage	2.96
Horizontal tail	3.18
Vertical tail	1.27
Booms x 2	1.5

3.3.2 Zero-Lift Drag Coefficient

The total zero-lift drag coefficient includes the contribution from individual components of the aircraft exposed to the atmosphere, interference effects on adjacent components and so on. The analytic computation of all these effects to produce a very accurate result is a seemingly difficult task. Instead a procedure which ensures near accurate results with minimal complications was adopted. In that procedure, the contribution of zero-lift drag coefficient from major air-exposed components of the aircraft were obtained and they were summed up and multiplied by a suitable correction factor to yield the final result.

Wing, Horizontal Tail and Vertical Tail

Zero-lift drag coefficient of the wing ($C_{D_{ow}}$) is evaluated using the expression

$$C_{D_{ow}} = C_{f_w} f_{tc_w} f_M \left(\frac{S_{wetw}}{S} \right) \left(\frac{C_{D_{min_w}}}{0.004} \right)^{0.4} \quad (3.29)$$

where

$$C_{f_w} = \frac{0.455}{\log_{10}(Re_w)^{2.58}} \quad (3.30)$$

$$Re_w = \frac{\rho V L}{\mu} \quad (3.31)$$

$$f_{tc_w} = 1 + 2.7(t/c)_{max} + 100(t/c)_{max}^4 \quad (3.32)$$

$$f_M = 1 - 0.08M^{1.45} \quad (3.33)$$

$$C_{D_{ow}} = C_{f_w} f_{tc_w} f_M \left(\frac{S_{wetplf}}{S} \right) \left(\frac{C_{D_{min_w}}}{0.004} \right)^{0.4} \quad (3.34)$$

$$(3.35)$$

For evaluating the Reynold's number (Re_w) over the wing, the characteristic length was chosen as the mean chord of the wing (\bar{c}). Assuming the density to be at the cruise altitude of 5 km, and dynamic viscosity at that altitude to be 1.628×10^{-5} , Re_w turns out to be 1.08×10^6 . Since it exceeds the critical Reynold's number of 5×10^5 from experience for a flat plate, majority of the flow was assumed to be turbulent in nature. This is also a better approximation since overestimation of drag is much better than its underestimation. The C_{f_w} relation used here holds only for turbulent flows. For laminar flows, the relation used is

$$C_{f_w} = \frac{1.327}{\sqrt{Re_w}} \quad (3.36)$$

The functional parameter f_{tc_w} depends on the maximum thickness to chord ratio of the airfoil as can be seen from the relation. The UAV operates in low subsonic range and the Mach number (M) is very less (0.08). Hence the parameter f_M can be approximated to 1. In the expression for $C_{D_{ow}}$, $C_{D_{min_w}}$ is obtained from the airfoil data of Cl vs Cd plot. The minimum drag coefficient as observed from this plot is used as the $C_{D_{min_w}}$ value. For the estimation of zero-lift drag coefficients for the tail surfaces, similar formula as compared to the wing section is

used.

$$C_{D_{o_{ht}}} = C_{f_{ht}} f_{t_{c_{ht}}} f_M \left(\frac{S_{wet_{ht}}}{S} \right) \left(\frac{C_{D_{min_{ht}}}}{0.004} \right)^{0.4} \quad (3.37)$$

$$C_{D_{o_{vt}}} = C_{f_{vt}} f_{t_{c_{vt}}} f_M \left(\frac{S_{wet_{vt}}}{S} \right) \left(\frac{C_{D_{min_{vt}}}}{0.004} \right)^{0.4} \quad (3.38)$$

$$(3.39)$$

Note that for the horizontal tail and vertical tail, their respective MACs are as the characteristic length in the evaluation of their Reynold's numbers.

Fuselage

For finding the zero-lift drag coefficient of the fuselage, the following formula is used:

$$C_{D_{o_f}} = C_{f_f} f_{ld} f_M \left(\frac{S_{wet_{fus}}}{S} \right) \quad (3.40)$$

The skin friction coefficient of the fuselage, C_{f_f} is a non-dimensional number and is defined the same way as C_{f_w} , but instead of Re_w , Re_f was used, which can be expressed as:

$$Re_w = \frac{\rho V L_f}{\mu} \quad (3.41)$$

Here L_f was taken as the length of the fuselage. Also the assumption of fully turbulent flow was used here as well. So C_{f_f} expression for turbulent flow was used. f_{ld} is a function of fuselage length-to-diameter ratio and was evaluated using

$$f_{ld} = 1 + \frac{60}{\lambda_f^3} + 0.0025 \lambda_f \quad (3.42)$$

where λ_f is the fuselage length-to-diameter ratio. Equivalent diameter was used here as the fuselage cross-section shape and size may vary across its length.

3.3.3 Overall C_{D_o}

Unaccounted factors may lead to a 50% increase in the total sum of the individual drag contributions. In order to compensate this issue, the overall C_{D_o} is expressed as:

$$C_{D_o} = K_c [C_{D_o} + C_{D_o} + C_{D_o} + C_{D_o} + \dots] \quad (3.43)$$

where K_c denotes a correction factor. For general aviation type aircraft, recommended value of 1.2 for K_c is used. Using this yields an overall C_{D_o} of 0.0376. The results obtained in the previous calculations are summarized in Table 3.4.

Table 3.4: Results of Zero-lift drag calculation

Component	C_{D_o}
Wing	0.0210
Fuselage	0.00230
Horizontal tail	0.00586
Vertical tail	0.00216
Overall	0.0376

3.4 Geometric Sizing

3.4.1 Wing Sizing

NACA 64418 was chosen as the airfoil for the wing based on comparing the wind tunnel data for different airfoils. It has the following characteristics:

Stall angle $\alpha_{stall} = 16^\circ$

Maximum lift coefficient $C_{L_{max}} = 1.4$

Zero lift angle of attack $\alpha_{L=0} = -3^\circ$

Airfoil lift curve slope $C_{l_\alpha} = 5.73/\text{rad}$

A trim angle (α_{trim}) of 7° and an aspect ratio (AR) of 8 was chosen for the subsequent design purposes. The low value of the aspect ratio was chosen by keeping in mind a relatively low wingspan so that the UAV can fly in confined spaces.

The following formula was used to obtain the C_{L_α} for the 3D wing from the C_{l_α} of the 2D airfoil.

$$C_{L_\alpha} = \frac{C_{l_\alpha}}{1 + \frac{C_{l_\alpha}}{\pi e AR}} \quad (3.44)$$

The ‘e’ in the equation, Oswald’s efficiency factor was obtained from this relation -

$$e = 1.78(1 - 0.045AR^{0.68}) - 0.64 \quad (3.45)$$

The obtained $C_{L\alpha}$ when used in the following relation yields the design lift coefficient.

$$C_L = C_{L\alpha}(\alpha_{trim} - \alpha_{L=0}) \quad (3.46)$$

As part of the geometric sizing of the aircraft wing, an initial span of 5 m was chosen.

Using the relation $AR = \frac{b^2}{S}$, the wing area $S = 3.125 \text{ m}^2$.

Using this wing area in the cruise velocity relation,

$$(3.47)$$

yielded $V = 40.48 \text{ m/s}$. Since this value exceeded the maximum permissible velocity of the aircraft (25-30 m/s), a span of 7 m was used instead, which yielded $S = 6.825 \text{ m}^2$ and $V = 28.92 \text{ m/s}$ which was within the acceptable limits of the aircraft velocity.

A 60% rectangular and 40% tapered wing was chosen with a taper ratio (λ) of 0.68 for the wing with the aid of historical data.

$$\bar{c} = \frac{b}{AR} \quad (3.48)$$

$$c_r = \frac{2S}{b(1 + \lambda)} \quad (3.49)$$

$$c_t = \lambda c_r \quad (3.50)$$

The above three relations yielded the mean aerodynamic chord $\bar{c} = 0.875 \text{ m}$, root chord $c_r = 1.042 \text{ m}$ and tip chord $c_t = 0.71 \text{ m}$.

3.4.2 Fuselage Design

Fuselage is an important component of an aircraft as it houses and protects the payload and control system and integrates other major components like the wing and the empennage. Generic external shape for different categories of aircrafts were taken under consideration and the fuselage type for a lightweight GA aircraft was chosen for the UAV. From the comparative analysis, the length of the aircraft was found to vary from 3 m to 5.5 m, with the average length of the aircraft estimated to be 3.85 m. Since the UAV utilizes pusher propellers, the length of the fuselage is reduced. As a first approximation in preliminary phase, the fuselage length was assumed to be $\frac{2^{rd}}{3}$ of the average length which was found to be 2.57 m.

3.4.3 Horizontal Tail Sizing

For the horizontal tail sizing, the following parameters were assumed:

$$\begin{aligned}V_H &= 0.6 \\ \lambda_{HT} &= 0.6 \\ S_{HT} &= 1.5 \text{ m}^2\end{aligned}$$

Then using the relations listed below, aspect ratio, l_t , and other geometric parameters of the horizontal tail were determined. The calculated parameters are listed in Table 3.

$$AR_{HT} = \frac{2}{3}AR \quad (3.51)$$

$$V_H = \frac{S_{HT}l_t}{S_{\bar{c}}} \quad (3.52)$$

$$b_{HT} = \sqrt{AR_{HT}S_{HT}} \quad (3.53)$$

$$c_{r_{HT}} = \frac{2S_{HT}}{b_{HT}(1 + \lambda_{HT})} \quad (3.54)$$

$$c_{\bar{H}T} = \frac{2}{3}c_{r_{HT}} \frac{1 + \lambda + \lambda^2}{1 + \lambda} \quad (3.55)$$

$$c_{t_{HT}} = \lambda_{HT}c_{r_{HT}} \quad (3.56)$$

3.4.4 Vertical Tail Sizing

The following were assumed -

Vertical tail area $S_{VT} = 0.6 \text{ m}^2$

Taper ratio $\lambda_{VT} = 0.6$

Aspect ratio $AR_{VT} = 1$

The following equations were used to obtain the relevant geometrical parameters of the vertical tail. Obtained results are depicted in Table 3.

$$V_V = \frac{S_{VT}l_t}{Sb} \quad (3.57)$$

$$b_{VT} = \sqrt{AR_{VT}S_{VT}} \quad (3.58)$$

$$c_{r_{VT}} = \frac{2S_{VT}}{b_{VT}(1 + \lambda_{VT})} \quad (3.59)$$

$$c_{\bar{V}T} = \frac{2}{3}c_{r_{VT}} \frac{1 + \lambda + \lambda^2}{1 + \lambda} \quad (3.60)$$

$$c_{t_{VT}} = \lambda_{VT}c_{r_{VT}} \quad (3.61)$$

Table 3.5: Design parameters

AR_w	7.18	AR_{HT}	4.79	AR_{VT}	1
b_w	7 m	b_{HT}	2.68 m	b_{VT}	0.77 m
\bar{c}_w	0.99 m	$c_{\bar{H}T}$	0.57 m	$c_{\bar{V}T}$	0.79m
c_{r_w}	1.16 m	$c_{r_{HT}}$	0.7 m	$c_{r_{VT}}$	0.97 m
c_{t_w}	0.789 m	$c_{t_{HT}}$	0.42 m	$c_{t_{VT}}$	0.58 m
		l_t	1.86 m		
		V_H	0.415 m		

3.5 Power Plant Selection

A nominal value of $C_{D_o} = 0.036$ was chosen and used in the following relations to obtain the required power.

$$k = \frac{1}{\pi e AR} \quad (3.62)$$

$$C_D = C_{D_o} + kC_L^2 \quad (3.63)$$

$$D = \frac{1}{2}\rho V^2 SC_D \quad (3.64)$$

$$P_{req} = DV \quad (3.65)$$

The power required was calculated to be 3.4 kW (or 4.56 hp) for the aircraft cruising at an altitude of 5 km. By taking the varying power requirements of the aircraft at different altitudes for different velocities into consideration, B150i UAV EFI engine system was selected as the power plant of choice out of the other shortlisted power plants. The engine characteristics are listed in Table 3.6.

Table 3.6: Engine characteristics for the fixed-wing mode

Engine type	Force air-cooled 2-stroke twin
Displacement	150 cc (9.15 ci)
Weight	4.3 kg
Power (7000 RPM)	7.5 kW (10 hp)
BSFC (5000-7000 RPM)	470 g/kW-hr (0.78 lb/hp-hr)
Fuel type	Gasoline, 50:1 premix

For the VTOL mode, thrust loading of 1.4 and climb velocity of 5 m/s was chosen[8].

$$\frac{T}{W} = 1.4 \quad (3.66)$$

$$P_{req} = TV_{climb} \quad (3.67)$$

The power required for the propotor was calculated to be 10.29 kW. Hirth 42 series 4201 engine was chosen for the design. Its characteristics are mentioned in Table 3.7.

Table 3.7: Engine characteristics for the VTOL mode

Engine type	Two cylinder two stroke (opposed)
Displacement	183 cc (11.5 ci)
Weight	5.7 kg
Power (6500 RPM)	11 kW (15 hp)
Dimensions	213 mm x 330 mm x 160 mm
Fuel type	Gasoline, 50:1 premix

3.6 Propeller Selection

Rotational speed $N = 3500 \text{ RPM}$ at 60% throttle at the cruise altitude of 5 km.

$$THP = \frac{P_{req}}{1000} \text{ kW} \quad (3.68)$$

$$BHP = \frac{THP}{\eta_p} \text{ kW} \quad (3.69)$$

Speed power coefficient can be obtained from the above parameters using the relation

$$C_s = V \left(\frac{\rho}{BHP n^2} \right)^{\frac{1}{5}} = 0.94 \quad (3.70)$$

where $n = N/60$.

For the obtained value of C_s , the following design chart was used to arrive at the pitch angle, propeller efficiency and advance ratio.

$$\begin{aligned}
 \text{Pitch angle } \beta &= 15^\circ \\
 \text{Propeller efficiency } \eta_p &= 0.73 \\
 \text{Advance ratio } J &= 0.5 \\
 \text{Diameter } d &= \frac{V}{nJ} = 0.94 \text{ m or } 36.96 \text{ in} \\
 \text{Pitch} &= \frac{V}{n} = 0.47 \text{ m or } 18.48 \text{ in}
 \end{aligned}$$

Based on the obtained diameter and pitch, Xoar 36x18 was chosen for the design from shortlisted propellers.

3.7 Control Surface Sizing

The guidelines for control surface sizing were obtained from Sadraey M.H. [1]. Table 3.8 shows the results obtained.

Table 3.8: Results of Control Surface Sizing

Control surface	Area (m^2)	Span (m)	Chord (m)	Inner edge location (m)
Aileron	0.34	1.40	0.13	4.20
Elevator	0.22	2.26	0.11	-
Rudder	0.09	0.54	0.12	-

Table 3.9: Maximum deflections

Control surface	Maximum deflection +ve (deg)	Maximum deflection -ve (deg)
Aileron	20 (down)	-25 (up)
Elevator	20 (down)	-25 (up)
Rudder	30 (left)	-30 (right)

3.8 Stability and Control Derivatives

Table 3.10: Summary of Longitudinal Stability and Control Derivatives

C_{L_o}	0.1859
C_{D_o}	0.376
C_{m_o}	0.08
C_{L_α}	4.7451
C_{m_α}	-0.4745
C_{L_q}	-3.3237
$C_{L_{\delta_e}}$	0.4732
C_{m_q}	-6.0698
$C_{m_{\delta_a}}$	-0.8642

Table 3.11: Summary of Lateral Stability and Control Derivatives

C_{Y_β}	-0.328
C_{l_β}	-0.189
C_{n_β}	0.028
C_{Y_p}	0.027
C_{l_p}	-0.674
C_{n_p}	-0.098
C_{Y_r}	0.224
C_{l_r}	0.195
C_{n_r}	-0.074

3.9 Trim Analysis

Figure 3.1: Lateral mode

Pole	Damping	Frequency (rad/TimeUnit)	Time Constant (TimeUnit)
-2.99e+00 + 1.27e+00i	9.20e-01	3.25e+00	3.35e-01
-2.99e+00 - 1.27e+00i	9.20e-01	3.25e+00	3.35e-01
-4.20e-03 + 1.68e-01i	2.50e-02	1.68e-01	2.38e+02
-4.20e-03 - 1.68e-01i	2.50e-02	1.68e-01	2.38e+02

Pole	Damping	Frequency (rad/TimeUnit)	Time Constant (TimeUnit)
-6.59e+00	1.00e+00	6.59e+00	1.52e-01
-8.25e-02 + 3.83e+00i	2.15e-02	3.83e+00	1.21e+01
-8.25e-02 - 3.83e+00i	2.15e-02	3.83e+00	1.21e+01
-8.24e-02	1.00e+00	8.24e-02	1.21e+01

Figure 3.2: Longitudinal mode

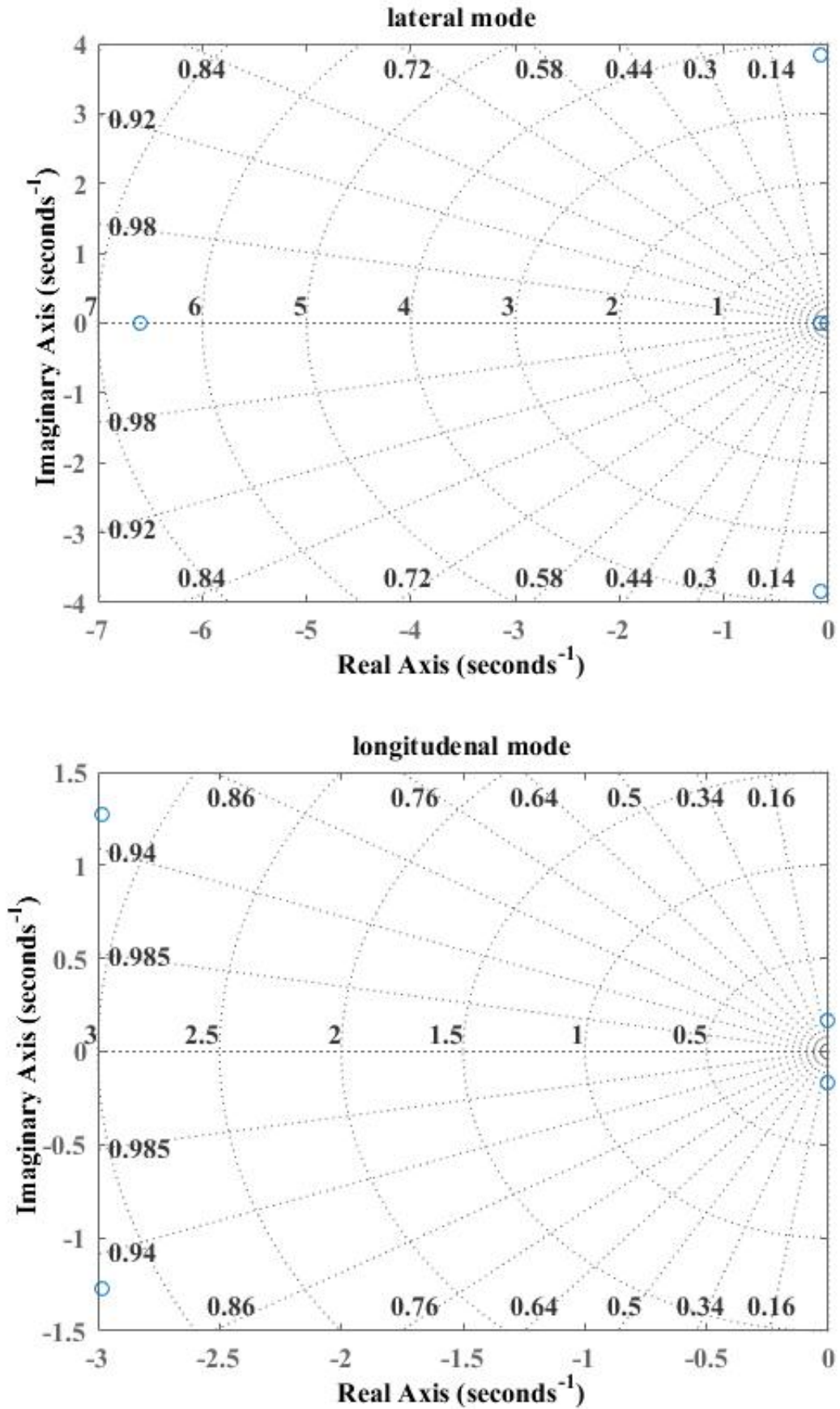


Figure 3.3: Performance Variation with Altitude

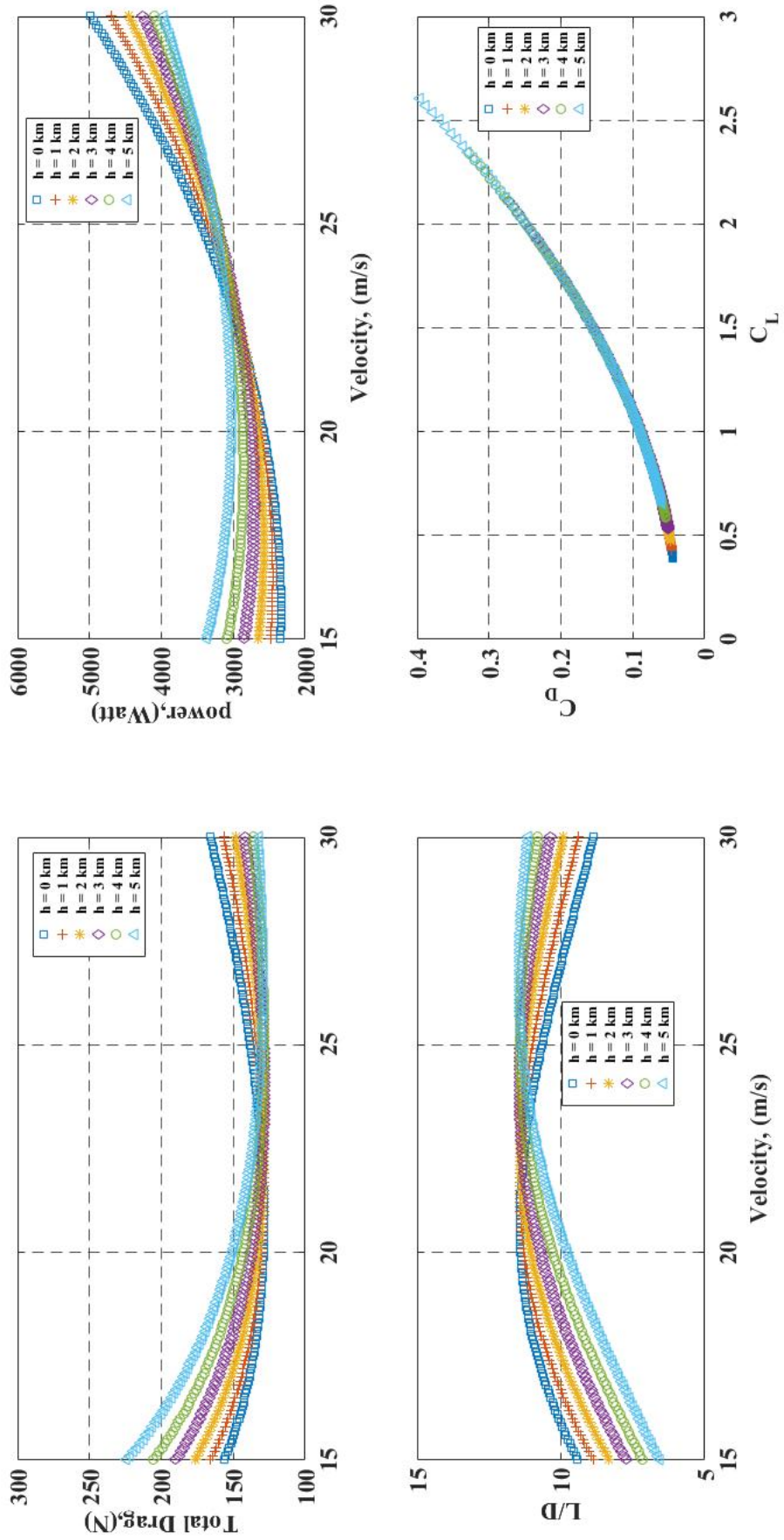
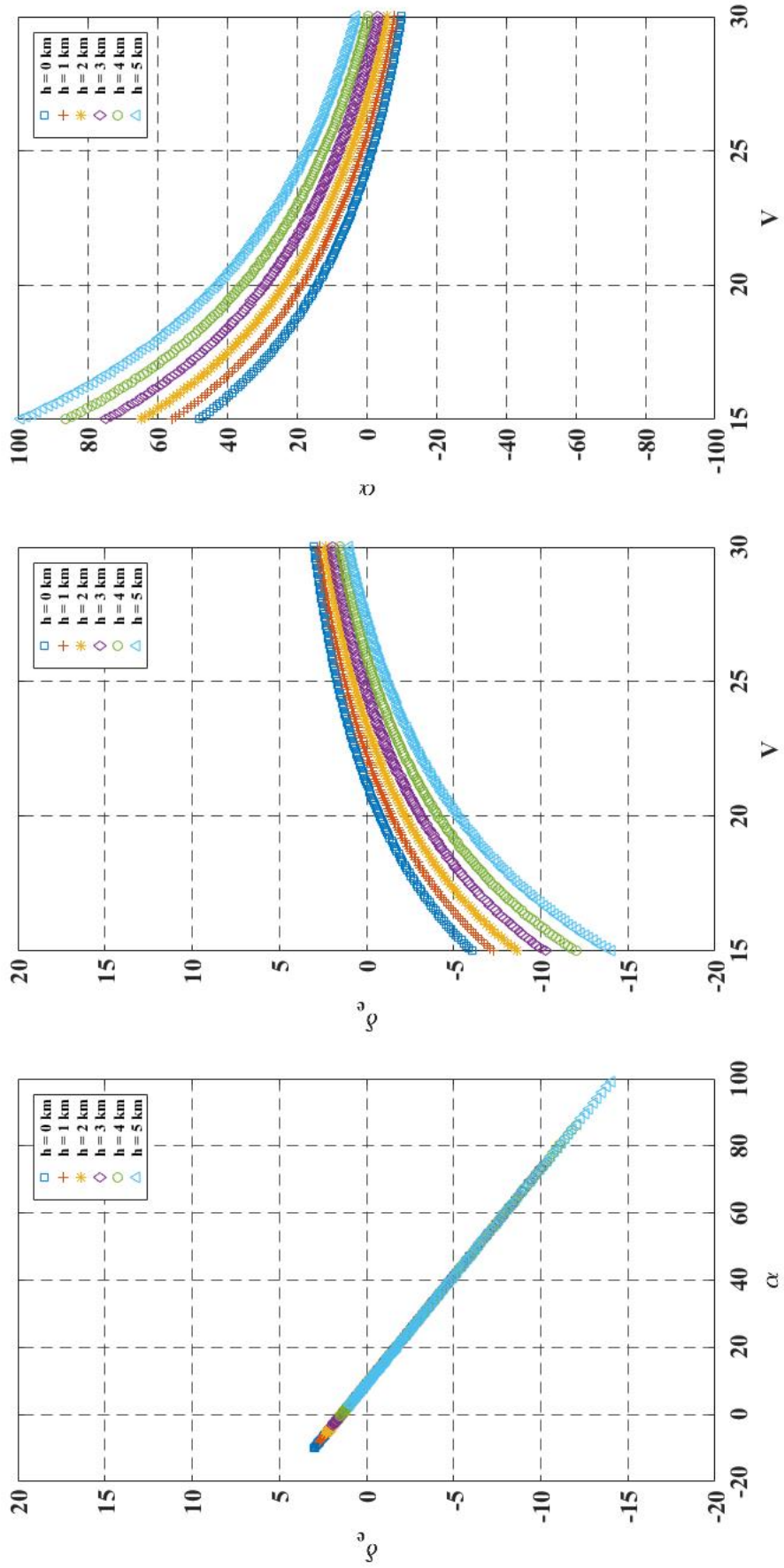


Figure 3.4: Trim Analysis with Altitude



Chapter 4

Spin Recovery

4.1 Introduction

Spin recovery analysis for the VTOL-UAV provides an important perspective about the effectiveness of some of its control surfaces.

Two methods were used for the purpose - the one recommended by Raymer book and the one described in Sadraey's book. For evaluating the spin characteristics of the aircraft, the method suggested by D. Raymer involved the estimation of the tail damping power factor (TDPF), relative density factor and the inertial yawing-moment parameter. These parameters were then used in an empirically estimated plot of spin recovery criteria 4.2 to check whether the UAV lies within the satisfactory region for both rudder alone recovery and rudder and elevator recovery.

4.2 Method I

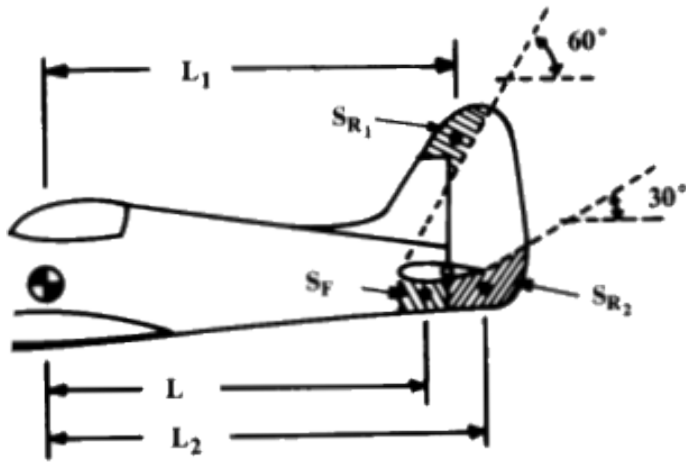
For evaluating TDPF, tail damping ratio (TDR) and unshielded rudder volume coefficient (URVC) were determined at first.

$$TDR = \frac{S_F L^2}{S_w \left(\frac{b}{2}\right)^2} \quad (4.1)$$

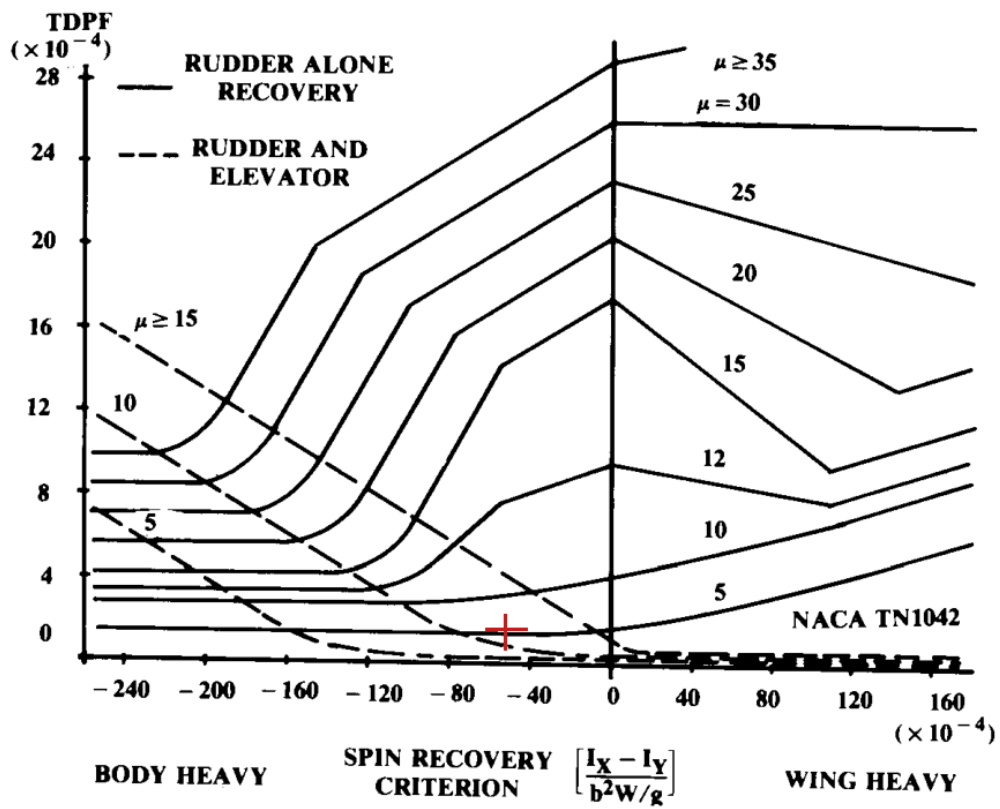
$$URVC = \frac{S_{R_1} L_1 + S_{R_2} L_2}{S_w \left(\frac{b}{2}\right)} \quad (4.2)$$

$$TDPF = (TDR)(URVC) \quad (4.3)$$

$$(4.4)$$



Source: Aircraft Design, D. Raymer



Source: Aircraft Design, D. Raymer

Relative density factor and inertial yawing moment parameters were calculated using these equations.

$$\mu = \frac{\left(\frac{W}{S}\right)}{\rho g b} \quad (4.5)$$

$$IYMP = \frac{I_X - I_Y}{b^2 \left(\frac{W}{g}\right)} \quad (4.6)$$

The value obtained for the relative density factor was 4.27 and the inertial yawing moment parameter was found to be -55×10^{-4} . The TDPF was close to 1.7×10^{-4} . These values were used in the empirical plot to verify that the UAV was spin-recoverable.

4.3 Method II

Sadraey's book mentions a process for the evaluation of maximum rudder deflection needed for the aircraft spin recovery. Required recovery yawing moment in stable spin is compared with maximum possible recovery yawing moment by rudder deflection. So, the required recovery yawing moment was estimated using

$$N_{SR} = \frac{I_{xx}I_{zz} - I_{xz}^2}{I_{xx}R_{SR}} \quad (4.7)$$

Maximum rudder deflection is typically about 30° for aircrafts comparable to the UAV under consideration. Rudder deflection for the above yawing moment was computed using

$$\delta_r = \frac{N_{SR}}{\frac{1}{2}\rho V_s^2 S b C_{n\delta_r}} \quad (4.8)$$

The rudder deflection angle obtained was equal to 34° . Since it is close to the maximum possible value of 30° from control surface sizing section, feasibility of the design for spin recovery was verified for situations requiring lower rudder deflections. With the modification of vertical tail from conventional configuration to boom mounted twin tail configuration, more pitching moment can be generated with lesser rudder deflection.

Chapter 5

Parachute Recovery System Design

5.1 Introduction

Although the preferred means of recovery/landing of the UAV is through the VTOL mode, the possibility of failure of some components and subsequent crash landing cannot be neglected while ensuring the overall safety of the vehicle. For such emergency purposes, recovery of the UAV can be made possible by using a parachute recovery system.

5.2 Material selection

Ripstop nylon was the chosen material for the parachute canopy. It is a lightweight nylon fabric interwoven with reinforcement threads. It is waterproof, water resistant, fire resistant and has very little porosity. Commercially available consumer grade ripstop parachute fabric weighs $0.045\text{kg}/\text{m}^2$.

Shroud lines and harnesses should be lightweight and it should maintain considerable strength. Nylon, polyester, Spectra, Vectran and Kevlar are some examples of commonly used materials for this purpose. Kevlar is a popular choice but Spectra has its own advantages over it. Spectra is as strong as Kevlar, but 15% lighter. It is abrasion resistant, tangle resistant, moisture resistant and costs the same as Kevlar. Hence Spectra was chosen as the material for shroud lines and harnesses.

5.3 Design

Parachutes can either act as pure drag devices or can be used for gliding. The primary objective of designing a PRS for the UAV here is for emergency recovery and hence it should act as a pure drag device. Such a system would reach a steady-state descent velocity when the gross aircraft weight is in equilibrium with parachute drag. Here it is assumed that the UAV drag is negligible compared to the parachute drag. The equilibrium relation will then be

$$W_{recov} = D = \frac{1}{2}\rho V_T^2 C_{D,Chute} S_{Chute} \quad (5.1)$$

$C_{D,Chute}$ is the drag coefficient of the parachute and S_{Chute} is the reference area of the parachute which is obtained by the projection of its surface to an observer above it. $C_{D,Chute}$ has a value that ranges from 0.7-1.47 for round parachutes. If D_{Chute} denotes the maximum diameter of the round parachute, then S_{Chute} can be expressed as

$$S_{Chute} = \frac{\pi}{4} D_{Chute}^2 \quad (5.2)$$

A descent velocity of 5 m/s and $C_{D,Chute}$ of 1 was assumed to obtain the parachute diameter from the relation

$$D_{Chute} = \sqrt{\frac{8W_{recov}}{\pi\rho V_T^2 C_{D,Chute}}} \quad (5.3)$$

The calculations yield the diameter of the projected area of the canopy D_{Chute} to be 5.73 m for parachute recovery load $W_{recov} = 25$ kg and terminal velocity of descent $V_T = 5$ m/s. Assuming a hemispherical canopy, its weight is calculated as

$$W_{canopy} = 0.045 \times 2 \times \frac{\pi}{4} D^2 \quad (5.4)$$

It comes out to be 2.32 kg.

Assuming a maximum opening shock value of 15g and a safety factor of 1.5, the design maximum load while deploying the parachute is calculated as

$$Load_{max} = 1.5 \times 15g \times W_{TO} \quad (5.5)$$

$$= 33,075.5 N \quad (5.6)$$

Suspension lines of type III paracord made of Nylon Kernmantle rope has a minimum breaking strength of 2440 N. With a fail-safe design in mind, a minimum of 18 suspension lines could be used. Type III paracord has a specific weight of 6.59 g/m. The length of the suspension lines should be such that it doesn't affect the proper orientation of the canopy. Considering the length of each suspension line as 4 m, total weight of the suspension lines turn out to be 474.5 g.

A simple deployment system like drogue parachute is used here. The drag force generated by the drogue/pilot parachute provides the force to deploy the main parachute. The weight of the drogue system is evaluated using the expression:

$$W_{drogue} = 0.12(C_D A)_d + (0.28 \times 10^{-3})q_\infty(C_D A)_d^{3/2} \text{ in } N \quad (5.7)$$

$$= 1.12 \text{ N or} \quad (5.8)$$

$$= 114.3g \quad (5.9)$$

5.4 Other Considerations

To flatten the weave of the parachute and to lower its porosity without conceding any increase in weight, fabric calendaring can be employed. It will also help the parachutes to stay packed for long periods of time. No coating has to be applied on the parachute as it can result in its net weight gain (about 10%). It might also lead to the sticking of the parachute fabric and resist opening if it stays packed for a long time.

Chapter 6

SOTM Installation

SOTM or SATCOM-On-The-Move is a phrase used to denote the technology in which a mobile vehicle equipped with a satellite antenna is able to establish and maintain communication with a distant satellite even when it is non-stationary. Equipping an aircraft with a SOTM reaps its own merits and demerits. With SOTM, it becomes possible to send large quantities of data at high speeds across intercontinental range. Unlike V/UHF radios, SOTM is not limited by a line-of-sight range. Installation of an SOTM in an aircraft concedes drag penalty, gross weight gain, and additional sophistication to make the SOTM functional. An application of SOTM is in the military sector, especially at locations where terrestrial communication is limited or compromised and where reliable, secure, and fast modes of data transmission is a necessity.

The change in drag for the UAV with and without the installation of a surface mounted SOTM was to be determined as part of the project. For that purpose, a model SOTM was chosen after a brief market survey. The chosen model bears resemblance to *Micro Sat LM*, a product of *Get Sat* company. It has a cylindrical shape, size of 32 x 25.5 cm and weighs 7.6 kg.

$$Re_{avg} = \frac{\rho V (L_{fus} + C_{sotm})}{\mu} =$$
$$C_f = \frac{0.455}{\log_{10}(Re_{avg})^{2.58}}$$
$$C_{D_{o_{sotm}}} = \frac{S_{wet}}{S_{sotm_{theory}}} C_f$$

$$e = 1.78(1 - 0.045AR^{0.68}) - 0.64$$

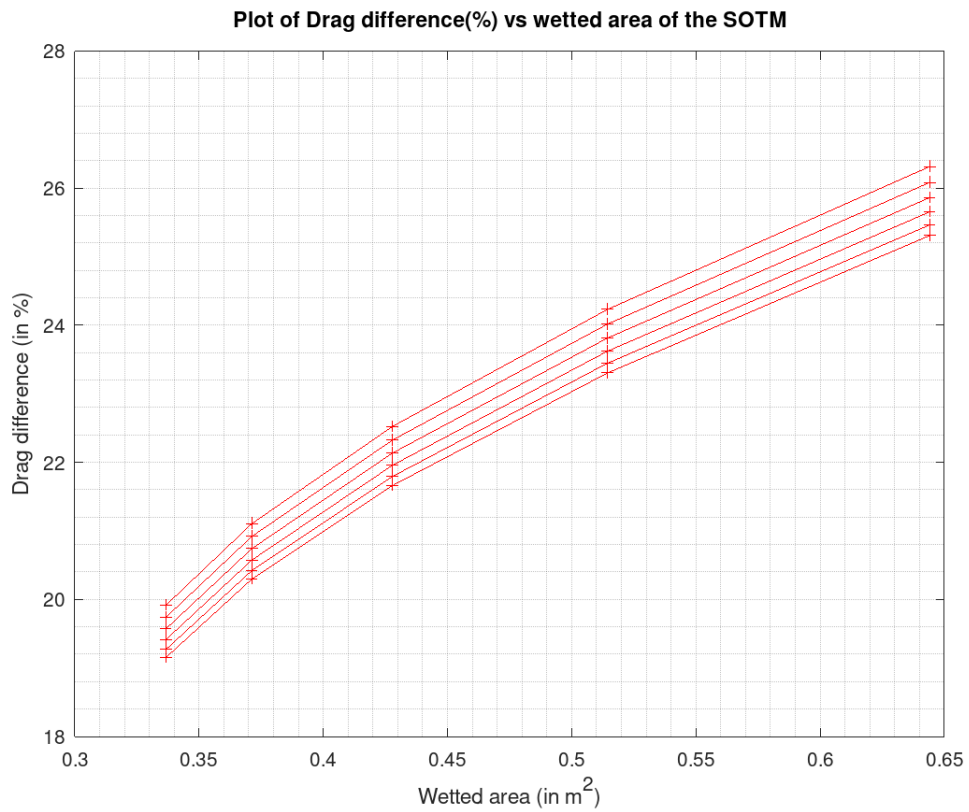
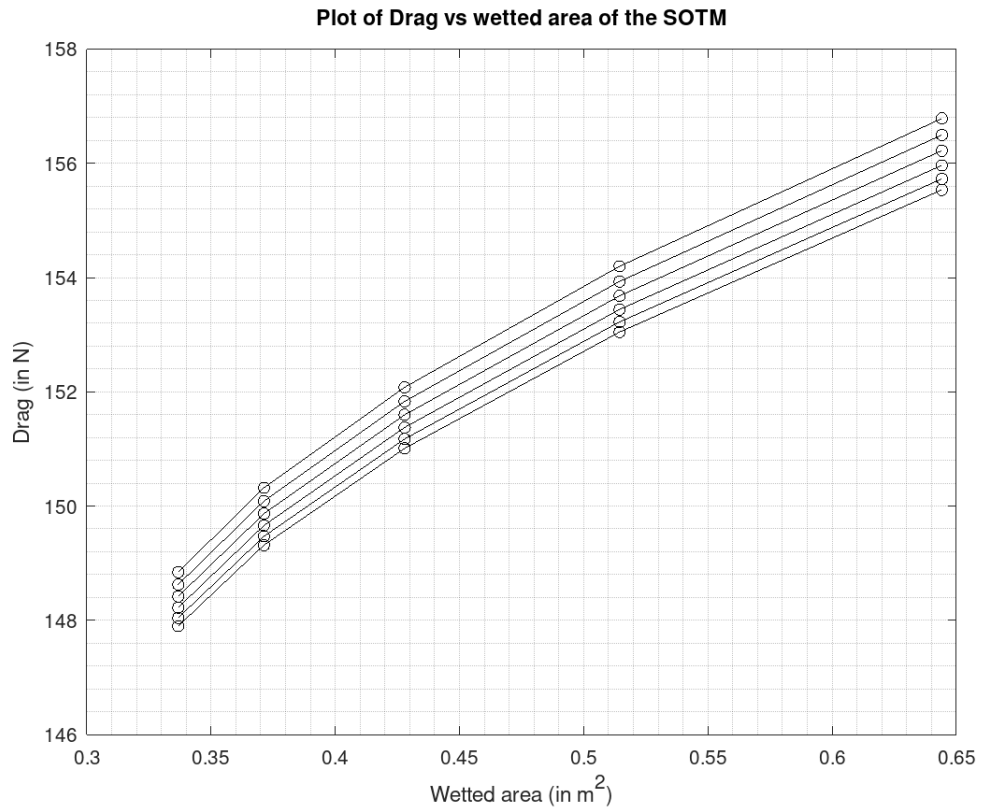
$$k = \frac{1}{\pi e AR}$$

$$C_{D_{new}} = C_{D_0} + C_{D_{O_{sotm}}} + kCL^2$$

$$D_{new} = C_{D_{new}} \frac{1}{2} \rho V_{cr}^2 S$$

$$P_{req_{new}} = D_{new} V_{cr}$$

Figure 6.1: Effects of Installation of SATCOM on the UAV



Chapter 7

Vn diagram, Wind and gust effects

7.1 Flight Envelope

From CS-VLA 335 regulations, maximum cruise speed cannot be less than

$$V_c = 2.4\sqrt{\frac{W_{TOG}}{S}} = 34.98 \text{ m/s} \quad (7.1)$$

$$(7.2)$$

maximum cruise speed is obtained from

$$V_{max} = 1.3V_c = 45.47 \text{ m/s} \quad (7.3)$$

$$(7.4)$$

Dive speed is taken as

$$V_d = 1.4V_c = 48.98 \text{ m/s} \quad (7.5)$$

$$(7.6)$$

For the wing, the values of $C_{L_{maxup}}$ was found to be 1.4 and $C_{L_{maxdown}}$ to be -0.9. Finding the stall speed for the UAV,

$$V_s = \sqrt{\frac{W_{TOG}}{\frac{1}{2}\rho_{sl}SC_{L_{maxup}}}} = 15.74 \text{ m/s} \quad (7.7)$$

$$(7.8)$$

The load factor variation was found to be varying with V in this quadratic form:

$$n = \frac{L}{W} = \frac{\frac{1}{2}\rho_{sl}SC_{L_{maxup}}}{W} = 0.004V^2 \quad (7.9)$$

$$(7.10)$$

Taking n_{pos} as 3.8 and n_{neg} as -1.9, maneuvering speed was calculated using:

$$V_{man} = \sqrt{n_{pos}/0.004} = 30.68 \text{ m/s} \quad (7.11)$$

Similar procedure was followed for the lower curve as well by replacing $C_{L_{maxup}}$ with $C_{L_{maxdown}}$ and n_{pos} with n_{neg} .

7.2 Wind and Gust effects

Gust Load factor variation during cruise flight

$$n = 1 + \frac{K_g V_{ge} V_e a \rho S_{wga}}{2W_{TO}} \quad (7.12)$$

$$(7.13)$$

where V_{ge} is taken as 25, 50 ft/s following CS-VLA regulations recommended for a low-subsonic UAV. The parameter a was estimated using

$$a = \frac{2\pi}{1 + \frac{2}{AR}} \quad (7.14)$$

$$(7.15)$$

Air vehicle mass aspect ratio was then evaluated:

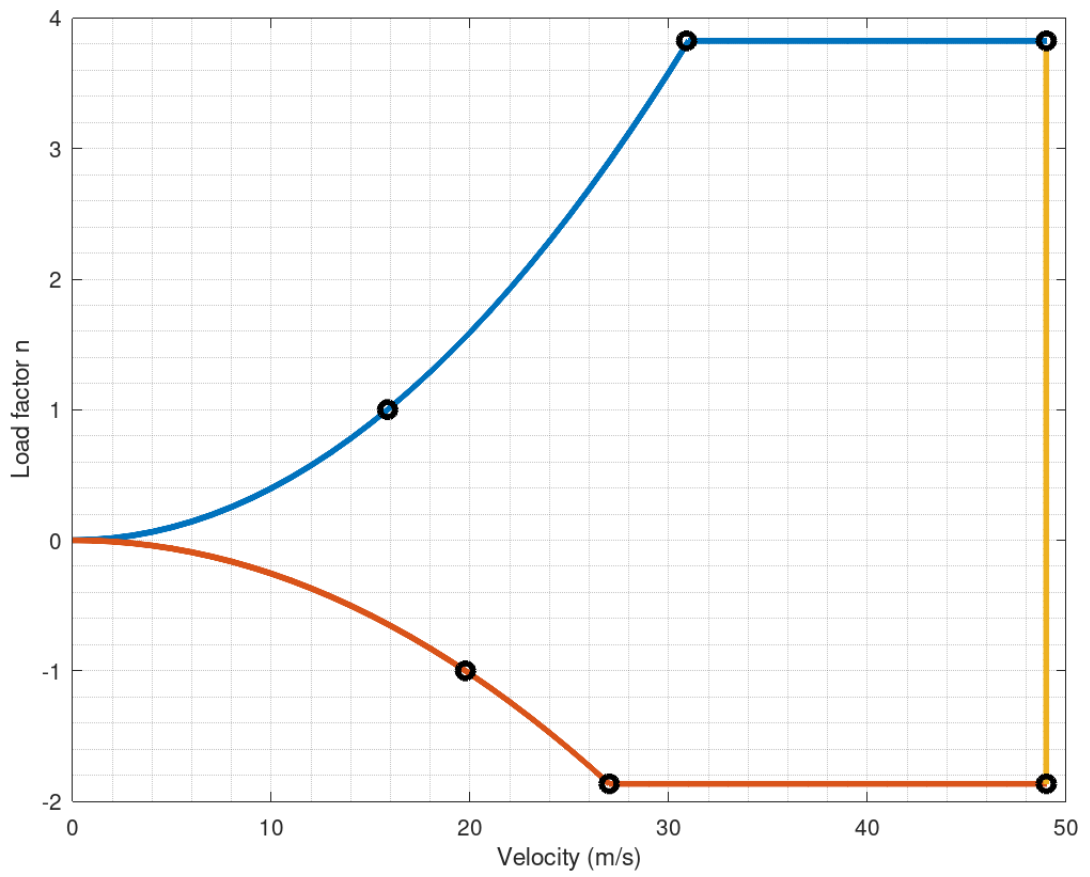
$$\mu_g = \frac{2W_{TO}}{\rho C_{mga} c S_{wga}} = \frac{2 \times 150}{0.736 \times 0.875 \times 5.026 \times 6.825} = 13.4 \quad (7.16)$$

Computing the gust alleviation factor K_g ,

$$K_g = \frac{0.88\mu_g}{5.3 + \mu_g} = \frac{0.88 \times 13.4}{5.3 + 13.4} = 0.63 \quad (7.17)$$

Inputting these values into equation 7.12 will yield a pair of straight lines. Following the same procedure for lower curves produces the required combined V-n diagram accounting for gust effects.

Flight envelope for the VTOL-UAV



Gust envelope for the VTOL-UAV

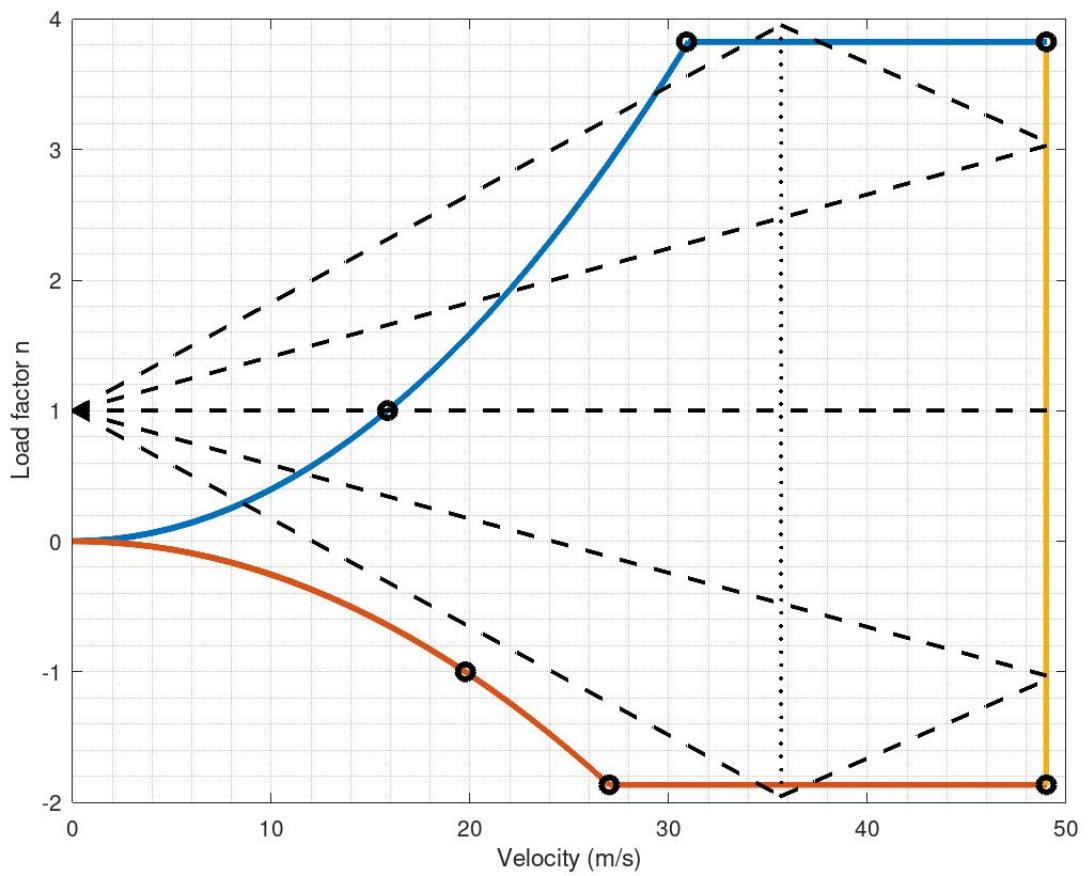


Figure 7.1: Orthographic Drawing

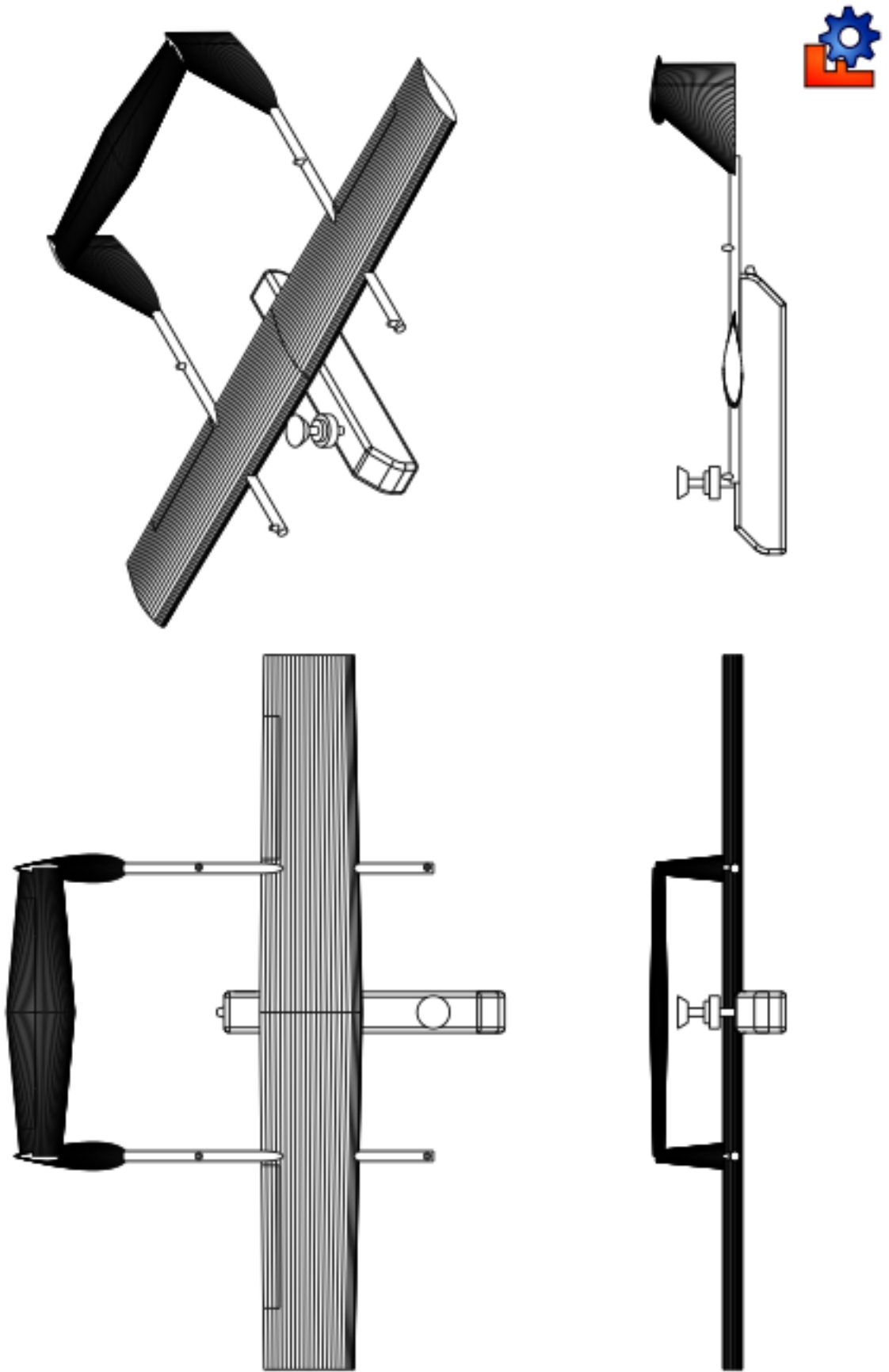
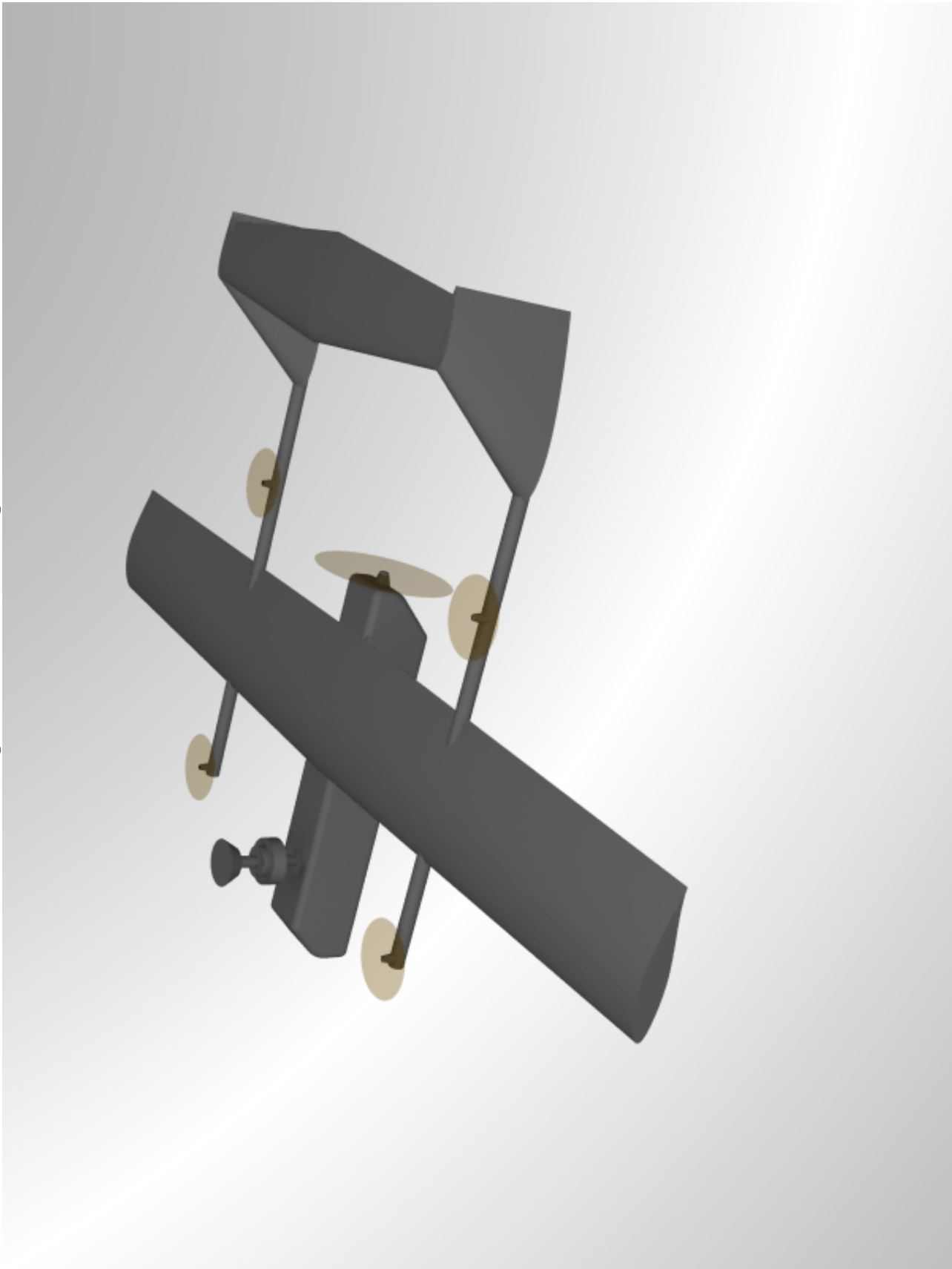


Figure 7.2: Rendered Image



Bibliography

- [1] Sadraey, M. H. (2013). *Aircraft design: a systems engineering approach*. Wiley, Chichester, West Sussex, U.K.
- [2] Gundlach J. (2012). *Designing Unmanned Aircraft Systems: Comprehensive Approach*. Reston: American Institute of Aeronautics and Astronautics.
- [3] Roskam, J. (1971) *Methods for Estimating Stability and Control Derivatives of Conventional Subsonic Airplanes*. Roskam Aviation and Engineering Corporation, Lawrence, Kansas.
- [4] Lyu, X., Gu, H., Zhou, J., Li, Z., Shen, S., & Zhang, F. (2018). *Simulation and flight experiments of a quadrotor tail-sitter vertical take-off and landing unmanned aerial vehicle with wide flight envelope*. International Journal of Micro Air Vehicles, 303–317. <https://doi.org/10.1177/1756829318813633>
- [5] Pankaj Pathak, Madhavi Damle, Parashu Ram Pal, Vikash Yadav, (2019). *Humanitarian Impact of Drones in Healthcare and Disaster Management*. International Journal of Recent Technology and Engineering (IJRTE) ISSN: 2277-3878, Volume-7 Issue-5.
- [6] Raymer, D. P., & American Institute of Aeronautics and Astronautics. (1989). *Aircraft design: A conceptual approach*. Washington, D.C: American Institute of Aeronautics and Astronautics.
- [7] *Power4flight B150i UAV engine system datasheet* <https://power4flight.com/wp-content/uploads/bsk-pdf-manager/2019/05/B150i-Datasheet-final.pdf>
- [8] *Hirth 42 series engine 4201 datasheet* <http://hirthengines.com/wp-content/uploads/4201-brochure-soft-copy.pdf>